UCRL--95843

DE87 011308

387

CONF-8607330--1


# DESIGN AND ANALYSIS OF A BROADBAND $TM_{01}$ MODE GENERATOR IN CYLINDRICAL WAVEGUIDE*


SCOTT C. BURKHART



THIS PAPER WAS PREPARED FOR SUBMITTAL TO

1987 2nd INTERNATIONAL MICROWAVE
SYMPOSIUM/BRAZIL
RIO DE JANEIRO, BRAZIL

JULY 27-30, 1986


Lawrence Livermore National Laboratory

# DESIGN AND ANALYSIS OF A BROADBAND $TM_{01}$ MODE GENERATOR IN CYLINDRICAL WAVEGUIDE

Scott Burkhart
Lawrence Livermore National Laboratory
P.O. Box 808
Livermore, CA 94550 USA

## ABSTRACT

A generator for launching the $TM_{01}$ mode in a cylindrical waveguide is described. Two-dimensional modeling demonstrated a mode purity ($TM_{02}/TM_{01}$ mode) in excess of 20 dB across most of the design 6-10 GHz. Testing of two fabricated generators showed that good mode purity was obtained in practice.

## INTRODUCTION

Many microwave generators currently being investigated generate their power in other than the commonly used $TE_{10}$ mode in rectangular waveguide. One common example is the gyrotron, where $TE_{01}$ and $TE_{02}$ cylindrical modes carry the power. Not so common, but being investigated in many laboratories, are relativistic magnetrons with axial extraction, backward wave oscillators, and virtual cathode oscillators. These generate $TM_{0n}$ modes in cylindrical waveguide. Many diagnostics have been developed to measure the $TM_{0n}$ modes, but they always depend on a pure mode generator for proper calibration. Therefore, the purpose of this paper is to develop the design of a well matched, broadband $TM_{01}$ generator that can generate a pure $TM_{01}$ mode in multimode waveguide.

## DESIGN

The design of the $TM_{01}$ mode generator can be broken down into six regions, as shown in Fig. 1. For each of the regions, we determined the outer conductor radius a(z), inner conductor radius b(z), and the overall length. This design was constrained by the 1.55 mm pin radius on the Type N input connector, an output waveguide radius of 42.5 mm, and a frequency range of 6.0 to 10.0 GHz.

The dimensions of Region III were determined first since the rest of the design revolved around Region III. The limitations on a and b imposed by the Marcuvitz[1] analysis were $1.14a < \lambda < 2.61a$. Given the 6-10 GHz frequency range, the constraint on a was $1.92 \text{ cm} < a < 2.63 \text{ cm}$. From Marcuvitz (Fig. 5.31-2,3),[1] the optimal choice for b/a is about 0.41, so choosing $b/a = 0.43$ is close to optimal, and also 50 Ω. Thus, we maintained 50 Ω all the way up to Section III. Setting the $TM_{02}$ cutoff ($k_c a = 5.52$) at 10.5 GHz for Section V, we obtained $a = 2.51$ cm. This is within the previously derived limits for a. The possibility of non-TEM coaxial modes is a consideration in Regions II and III and must be checked for. In a 50 Ω coaxial line that is kept azimuthally symmetric, the first spurious mode of concern is the $TM_{01}$ mode. Solving numerically for the cutoff frequency,[2] one obtains $k_c a = 5.504$ which yields an acceptable cutoff frequency of 10.5 GHz.

**MASTER**

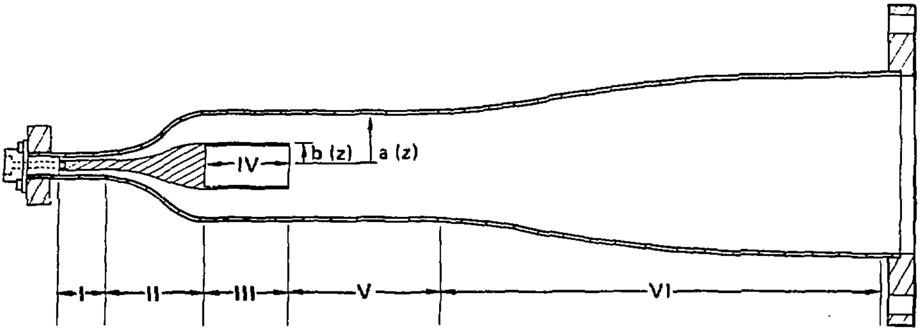


Figure 1. Side view of the $TM_{01}$ mode generator. The different design regions are denoted with numerals I through VI.

The design of Section I was relatively simple. The dimension b was chosen to be 2.13 mm, followed by a straight section which was continued for a distance of 9.8 mm to cut off any spurious modes before tapering in Section II. Section V was dimensioned using Eq. (3) to cause at least 30 dB attenuation of the evanescent $TM_{02}$ mode from the end of the center conductor to the beginning of the waveguide taper.

$$A = \text{attenuation (dB)} = 20 \log(e^{-\gamma z}) \tag{1}$$

$$\gamma = k_c^2 - k^2 \tag{2}$$

Solving for z in Eq. (1),

$$z = \frac{A}{20 \gamma \log e} \tag{3}$$

Solving Eq. (3) for the $TM_{02}$ mode at 10 GHz with a = 25.1 mm, we find that Section V must be at least 51.2 mm, so we chose it to be 60 mm. The length of Section IV was also chosen using Eq. (3), except that for Section IV we wanted the lowest order TM mode ($TM_{01}$) to be attenuated by at least 30 dB before it reached the left wall. The radius of Section IV was chosen to be 10.1 mm which left enough wall thickness. With the cutoff wavenumber $k_c = 2.405/a = 238.1$, and $k = 209.4$ as before, Eq. (3) yields $z = 30.5$ mm, so we chose 40 mm.

Sections II and VI were designed using tapered transition design techniques.[3-9] The coupling from the desired mode to the most closely coupled undesired mode is described by a distribution function over the length of the nonuniform waveguide section. The author chose to use the modified Dolph-Chebyshev distribution function,[4] also known as the modified sin x/x response function for taper Sections II and VI. There is a problem, however, when doing the usual taper design on Section II, because its impedance is 50 Ω throughout. A taper was therefore designed assuming that the inner conductor remained constant while the outer conductor tapered from 4.9 mm to 25.1 mm. The taper length was chosen to be $\beta L = 7$ which typically yields a good taper. The taper length is L, and $\beta = 1/2(\beta_1 - \beta_2)$, where $\beta_1$ and $\beta_2$ are respectively the wavenumbers of the desired mode, and the first spurious mode. For the Section II coaxial taper, the spurious mode is just the reflected TEM wave. Thus $\beta = \beta_1$, and the length must be at least 56 mm, so we chose it to be 60 mm. The inner conductor radius b(z) was chosen to obtain 50 Ω. Maintaining a constant cross section is very important in Section II to avoid trapping the $TM_{01}$ coaxial mode. As the coaxial line impedance increases, the $TM_{01}$ coaxial mode cutoff frequency decreases, approaching the hollow guide $TM_{01}$ value $k_c a = 2.405$.

The Section IV taper design was done using the $TM_{01}$ cylindrical mode as the desired mode, and the $TM_{02}$ mode as the spurious mode. Thus, $\beta_1 = 2.405/a$ and $\beta_2 = 5.52/a$. Hecken and Anuff[6] pointed out that mode reconversion must be taken into account when designing a taper between two very different waveguide sizes. Existing synthesis methods do not include mode reconversion, so what was done here was to synthesize a 35 dB taper at 12.5 GHz, then analyze it to verify that the $TM_{02}$ mode power was at least 40 dB below the $TM_{01}$ mode power from 6-10 GHz. The dimensions of the Section VI taper are listed in Table I. The Table II dimensions can be scaled to different frequency bands, except for Sections I and II which must observe the fixed dimensions of the input coaxial connector. The final design dimensions are all summarized in Table II.

## ANALYSIS

Marcuvitz[1] has an analysis of the $TM_{01}$ mode generator considering only Sections III-V and a vanishing thickness to the inner conductor shell in Section III. The analysis shows the coaxial-cylindrical waveguide junction to look like the junction of two transmission lines with different characteristic impedances $Z_1$ and $Z_2$.

$$\frac{Z_2}{Z_1} = \frac{\lambda_g}{\lambda} \tag{4}$$

The guide wavelength $\lambda_g$ refers to the $TM_{01}$ mode, and $\lambda$ is the free space wavelength. For a 25.1 mm radius waveguide, Eq. (4) predicts a return loss of 13.3 dB at 6 GHz, decreasing to 24.3 dB at 10 GHz. The transmitted power is claimed to be all converted to the $TM_{01}$ mode. However, in practice, some is converted to higher order modes as is shown by simulations and measurement.

The design was checked numerically by simulating it with a two-dimensional finite difference code. The geometry of the $TM_{01}$ mode generator is shown in Fig. 2 as it was simulated. A TEM wave with a linearly swept frequency was launched at the left-hand coaxial boundary. The output was measured just before the right waveguide boundary using 42 radial spaced electric and magnetic field sampling points. The sampled fields were expanded in a Fourier-Bessel series[10] in $J_1$, where $J_1$ is the Bessel function of the first kind of order one.

Table I. Section VI waveguide radius a(z) vs. the axial dimension z.

| z (mm) | a(z) (mm) | z (mm) | a(z) (mm) | z (mm) | a(z) (mm) |
|---|---|---|---|---|---|
| 0.0 | 25.1 | 80.0 | 34.07 | 160.0 | 41.11 |
| 10.0 | 25.32 | 90.0 | 35.39 | 170.0 | 41.50 |
| 20.0 | 25.87 | 100.0 | 36.58 | 180.0 | 41.81 |
| 30.0 | 26.82 | 110.0 | 37.64 | 190.0 | 42.06 |
| 40.0 | 28.10 | 120.0 | 38.56 | 200.0 | 42.24 |
| 50.0 | 29.58 | 130.0 | 39.36 | 210.0 | 42.37 |
| 60.0 | 31.12 | 140.0 | 40.05 | 220.0 | 42.46 |
| 70.0 | 32.64 | 150.0 | 40.63 | 230.0 | 42.50 |

Table II. Summary of the $TM_{01}$ mode generator design.

| Sec. | Design | | Sec. | Design | |
|---|---|---|---|---|---|
| I | length | - 25 mm | IV | length | - 40 mm |
| | outer radius | - 4.9 mm | | radius | - 10.1 mm |
| | inner radius | - 2.13 mm | V | length | - 60 mm |
| II | length | - 60 mm | | radius | - 25.1 mm |
| | outer radius | - 4.9 mm-25.1 mm | VI | length | - 230 mm |
| | inner radius | - 2.13 mm-10.9 mm | | radius | - 25.1 mm-42.5 mm |
| | taper dimensions | in Table I | | taper dimensions | in Table II |
| III | length | - 40 mm | | | |
| | outer radius | - 25.1 mm | | | |
| | inner radius | - 10.9 mm | | | |

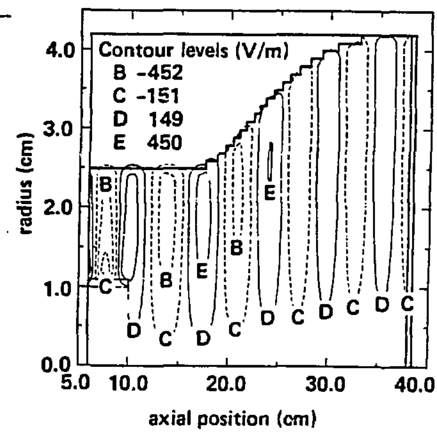


Figure 2. The $TM_{01}$ mode generator as simulated by the z-r finite difference code. The contours are equipotentials of the radial electric field.

The expansion allowed us to determine the mode content, which in this case consisted of a superposition of $TM_{0n}$ modes. The main unwanted mode to appear was the $TM_{02}$ mode, but it was kept to less than 20 dB below the $TM_{01}$ mode power for most of the band from 6-10 GHz as shown in Fig. 3.

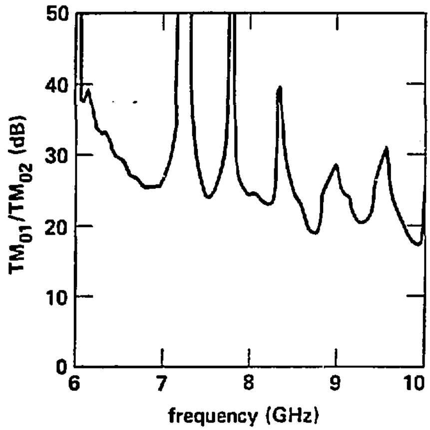


Figure 3. Ratio of the $TM_{01}/TM_{02}$ power as calculated by the simulation code. More than 20 dB between the two modes is calculated across most of the 6-10 GHz bandwidth.

## EXPERIMENTAL RESULTS

Two $TM_{01}$ generators were fabricated as summarized in Table II using electroform techniques. The mode conversion efficiency was then checked using several methods. In one method, short (1-10 ns) microwave pulses were injected into a long cylindrical waveguide using the $TM_{01}$ generator, and the pulse propagation was monitored with radial E-field probes. No pulse dispersion due to multi-moding was observed. The second method was to measure $|S_{21}|$ for two $TM_{01}$ generators connected back to back. Figure 4 shows $|S_{21}|$ from 5.5 to 10.5 GHz, only one spurious resonance appears, at 7.1 GHz. A 1 dB or less ripple appears over the rest of the band, which shows that the transmitted power remains in the $TM_{01}$ mode, with little mode conversion to the $TM_{02}$ mode. I attribute the 1 dB ripple to the teflon/air junction in Section I, which was not optimized for a good match. The spurious 7.1 GHz resonance is most likely due to $TM_{02}$ mode conversion, which could be due to the waveguide junction where the two $TM_{01}$ generators connect.

## ACKNOWLEDGMENT


I would like to thank L. Hangartner who worked with me on the mechanical details, which involved two different but equivalent designs. The work was supported by the U.S. Department of Energy under Contract No. W-7405-ENG-48.

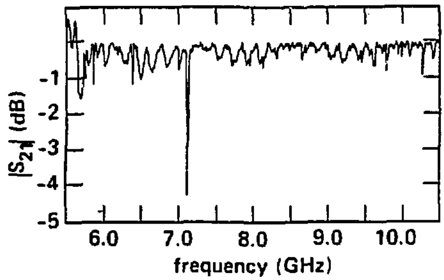


Figure 4. $|S_{21}|$ of two $TM_{01}$ mode generators connected back to back. One spurious resonance occurs at 7.2 GHz.

## REFERENCES


1. N. Marcuvitz, Waveguide Handbook, 1st Ed. (McGraw-Hill, New York, 1951), pp. 323-326.
2. S. Ramo, J. R. Whinnery, and T. Van Duzer, Fields and Waves in Communication Electronics, 1st Ed. (Wiley, New York, 1965), p. 446.
3. L. Solymar, "Spurious mode generation in nonuniform waveguide," IEEE Trans. Microwave Theory Tech., Vol. 7, pp. 379-383, July 1959.
4. R. P. Hecken, "A near optimum matching section without discontinuities," IEEE Trans. Microwave Theory Tech., Vol. MTT-20, pp. 734-739, Nov. 1972.
5. H. G. Ungar, "Circular waveguide taper of improved design," Bell Sys. Tech. J, Vol. 37, pp. 899-912, July 1958.
6. R. P. Hecken and A. Anuff, "On the optimum design of tapered waveguide transitions," IEEE Trans. Microwave Theory Tech., Vol. MTT-21, pp. 374-380, June 1973.
7. J. L. Doane, "Hyperbolic secant coupling in overmoded waveguide," IEEE Trans. Microwave Theory Tech., Vol. MTT-32, pp. 1362-1371, Oct. 1984.
8. R. E. Collin, "The optimum tapered transmission line matching section," Proc. IRE, Vol. 44, pp. 539-548, Apr. 1956.
9. F. Sporleder and H. G. Ungar, Waveguide tapers transitions and couplers. London: Institution of Elec. Eng., 1979.
10. J. D. Jackson, Classical Electrodynamics, (Wiley, New York, 1975) p. 109.



*This work was performed under the auspices of the U.S. Department of Energy by Lawrence Livermore Laboratory under contract No. W-7405-Eng-48.